Functional Box-Counting and Multiple Elliptical Dimensions in Rain

S. Lovejoy; D. Schertzer; A. A. Tsonis

Science, New Series, Vol. 235, No. 4792 (Feb. 27, 1987), 1036-1038.

Reports

Functional Box-Counting and Multiple Elliptical Dimensions in Rain

S. LOVEJOY, D. SCHERTZER,* A. A. TSONIS

Many physical systems that have interacting structures that span wide ranges in size involve substantial scale invariant (or scaling) subranges. In these regimes, the large and small scales are related by an operation that involves only the scale ratio. The system has no intrinsic characteristic size. In the atmosphere gravity causes differential stratification, so that the scale change involves new elliptical dimensions (d_{el}). Fields that are extremely variable, such as rain, involve multiple scaling and dimensions that characterize the increasingly intense regions. Elliptical dimensional sampling and functional box-counting have been used to analyze radar rain data to obtain both the multiple dimensions of the rain field and the estimate $d_{el} = 2.22 \pm 0.07$.

SOME TIME AGO, LOVEJOY (*1*) ANALYZED infrared satellite cloud pictures over a wide range of scales by fixing an infrared radiance threshold and measuring all the areas (A) and corresponding perimeters (P) of isolated regions that exceeded the threshold. Over the range from roughly 1 to 1000 km, a scaling relation of the form $P \propto A^{D/2}$ was obtained, where D is interpreted as the fractal dimension of the (complex) cloud perimeters. Over the narrow range of radiance thresholds examined (corresponding to cloud tops of roughly -5, -10, and -15°C), D was nearly constant ($\sim 1.35 \pm 0.05$).

Since then considerable progress has been made in our understanding of both scaling sets (where the only information of interest is whether a point belongs to a set) and scaling fields (in which a number is assigned to each point in space, for example, the temperature). Simple types of scaling, in which the large scale is a (statistically) magnified copy of the small scale (or "self-similarity"), are actually a special case. Differential atmospheric stratification and rotation (due to gravity and the Coriolis force, respectively) could be treated with a simple anisotropic scaling operation (*2–6*) that involved compression as well as magnification and could be characterized by "elliptical" dimensions (estimated to be 23/9 = 2.555 in the horizontal wind field). Later work (*7–10*) showed that general anisotropic (and even nonlinear) scalings were possible in the framework of a formalism called "generalized scale invariance." Scaling did not necessarily depend on the notion of distance; the scale could be defined by other notions of size, such as the volume of an average cloud. Another development was the recognition that scaling generally involves not one but an infinite sequence of fractal dimensions (*4–7, 9–14*). An immediate consequence is the dependence of scale and dimension on statistical averages, which has been empirically demonstrated in rain data (*15, 16*) [see also (*17, 18*) for the implications for inhomogeneous measuring networks].

For studying the atmosphere, the limited early results must be systematically extended to determine the diminishing dimensions of the increasingly intense (and therefore cold) cloud tops, as well as the differential stratification and rotation of clouds (associated with, for example, their "texture"). For this purpose the original A-P relation is of limited interest. First, the lower limit of the perimeter dimension is one, since it is a line. Hence it cannot be used to examine the very intense regions with $D < 1$. Second, it cannot easily be adapted for studying anisotropy. Finally, the perimeter has no obvious physical significance. We can now estimate the multiple dimensions directly with a new technique which we call functional "box-counting." This technique is simple, gives physically interesting results, and can easily be adapted to directly estimate the elliptical dimension that characterizes the degree of stratification.

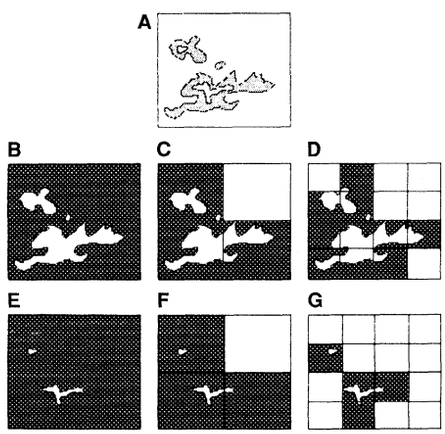

Fig. 1. Functional box-counting analysis of the field $f(r)$. In (**A**) the field is shown with two isolines that have threshold values $T_2 > T_1$; the box size is unity. In (**B**), (**C**), and (**D**), we cover areas whose value exceeds T_1 by boxes that decrease in size by factors of 2 and obtain $N_{T_1}(1) = 1$, $N_{T_1}(1/2) = 3$, and $N_{T_1}(1/4) = 10$, respectively. In (**E**), (**F**), and (**G**) we proceed in a similar manner for $T = T_2$, and obtain $N_{T_2}(1) = 1$, $N_{T_2}(1/2) = 3$, and $N_{T_2}(1/4) = 4$. Finally $D(T)$ is estimated with the equation $N_T(L) \propto L^{-D(T)}$.

The intuitive notion of the dimension (D) of a set of points (whether fractal or otherwise) is that the number $N(L)$ of disjoint squares (or cubes of appropriate dimension) of size L needed to completely cover the set varies as $N(L) \propto L^{-D}$. Numerical procedures called "box-counting algorithms" directly use this idea to estimate D [see, for example, (*11*)]. To obtain a functional version that is applicable, for example, to cloud or rain fields, we must first transform the function into an appropriate set of points. One way to do this (see Fig. 1) is to start with a function $f(r)$, where r is the position, that has a certain minimum resolution (in space or time) and then fix a threshold T. The set of interest is defined as the set of points such that $f(r) \geq T$. By varying T, we obtain the (decreasing) function $D(T)$. We assume that the process is fairly stationary, and that large values of f represent intense, rare events.

Rather than apply this method to cloud pictures [as in (*19*)], in this case we applied it to radar rain reflectivities. These reflectivities are probably the highest quality geophysical data available for this purpose. The raindrops are efficient natural tracers that allow the three-dimensional rain structure to be sampled quickly and without perturbation. The archives at the McGill weather radar observatory contain data that span over two orders of magnitude in each horizontal direction, one order of magnitude in the vertical direction, five orders of magnitude in time, and six orders of magnitude in intensity (the reflectivity, Z). The data we analyzed were resampled in coordinates (r, θ, z) (range, azimuth, and height above the earth's surface) instead of the original polar (r, θ, φ) coordinates with 200 by 375 by 8 resolution elements. The intensities were resolved into 16 logarithmic levels that were 4 dB apart (a factor of ~ 2.5). The entire scale therefore spans a range of $15 \times 4 = 60$ dB = factor of 10^6. Reflectivity levels in rain

S. Lovejoy and D. Schertzer, Physics Department, McGill University, Montreal, Quebec H3A 2T8.
A. A. Tsonis, Department of Geological and Geophysical Sciences, University of Wisconsin–Milwaukee, Milwaukee, WI 53201.

*Permanent address: Météorologie Nationale, 2 Avenue Rapp, Paris 75007, France.

can readily exceed the minimum detectable signal by a factor of 10^5.

Physically the reflectivity is the integrated backscatter of the raindrops. The microwave reflectivity for each drop is proportional to V^2 (where V is the raindrop volume). At the 10-cm wavelength used the absorption is sufficiently small so that the beam is nearly unattenuated. When Z is measured in this way, the integral over an entire "pulse" volume (roughly 1 km^3) of V^2 of each drop is modulated by its phase. Operational (meteorological) use of radar data is limited, because the rain rate (R) is a different integral, one over the product of V and the fall speed. The standard semiempirical relation between R and Z, which is only approximate, is called the Marshall-Palmer formula: $Z = 200\,R^{1.6}$ (with Z in millimeters to the sixth power per cubic meter, and R in millimeters per hour). By studying relative reflectivities directly, rather than studying R, we avoid the traditional radar calibration problem. Noise and instrumental biases are small.

When functional box-counting is applied to the radar-reflectivity data for a single radar scan, we obtain the results shown in Fig. 2, A and B. In the horizontal direction, we used sectorial (pie-shaped) boxes. The angular and downrange box sizes increased by factors of 2, and started with the highest resolution available (the use of pie-shaped boxes eliminates all range-dependent effects, such as beam spreading). The straightness of the lines shows that scaling is accurately followed in both horizontal and vertical directions. Note the systematic decrease in the absolute slope [which is $D(T)$] as T is increased (total range of reflectivity ~40,000). Out of 20 radar volume scans studied, all yielded fits of similar quality to those shown in Fig. 2, A and B. For greater values of T, $N(L)$ was too small to give reliable estimates of $D(T)$ (*20*) [for more applications of this technique, see (*19, 21*)].

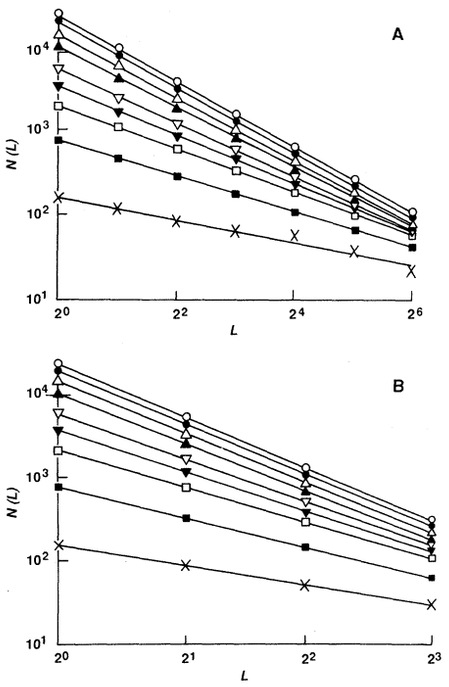

Fig. 2. (**A**) Plot of $N(L)$ versus L for the nine radar reflectivity thresholds described in the text, for a single radar volume scan, analyzed with horizontal boxes that increased by factors of 2 in linear scale. The different symbols indicate the thresholds that increased from top to bottom by 4 dB and started at 4 dB above the minimum detectable signal. The negative slope, $D_2(T)$, decreased from 1.24 to 0.40. (**B**) A similar analysis, except that the boxes used are cubical, and yielded values of $D_3(T)$ that decreased from 2.18 to 0.81. Only eight different vertical levels were available.

By applying functional box-counting to horizontal cross sections and volumes (using horizontal squares and cubes, respectively), we obtain the functions $D_2(T)$ and and $D_3(T)$ (Fig. 2, A and B). If the rain field is isotropic, then $D_3(T) = 1 + D_2(T)$; that is, taking cross sections reduces the dimension by one. This means that the codimensions $C_d(T)$ with respect to the embedding space dimension $d[C_d(T) = d - D_d(T)]$ are conserved:

$$C_3(T) = C_2(T) \qquad (1)$$

Equation 1 expresses the fact that at any scale L, the fraction $F_T(L)$ of either the plane or volume (more generally, of a space dimension d) covered by the fractal would be the same:

$$F_T(L) \sim L^{D_d(T)}/L^d = L^{-C_d(T)} \qquad (2)$$

However, atmospheric fields are not isotropic but stratified. In stratified anisotropic scaling, the average structures become flatter at larger and larger scales (as in Fig. 3); for example, for clouds of horizontal length L, the height is proportional to L^{h_z} (where h_z is an exponent that characterizes the degree of stratification). Hence the volume available for rain structures is L by L by $L^{h_z} = L^{d_{el}}$, where $d_{el} < 3$ is the "elliptical dimension" of the space (*2, 3, 5, 7, 10*), that characterizes the flattening. For completely stratified processes, $h_z = 0$ and $d_{el} = 2$; for isotropic fields, $h_z = 1$ and $d_{el} = 3$, as we expect. Since rain areas that exceed a fixed threshold ($T > 0$) do not fill all space, their "volume" increases as $L^{D_{el}(T)}$, with $D_{el}(T) < d_{el}$. However, if measured in the elliptical space in which the process occurs (*22*), the fraction occupied by the fractal at size L is the same as that of the two-dimensional (unstratified) cross section; hence the generalization of Eq. 1 is $C_{d_{el}}(T) = C_2(T)$. If an inappropriate box-counting space is used (defined as D_{el}), it can be shown (*10, 22*) that the correction D_{el}/d_{el} must be applied, which yields $C_{D_{el}}(T) = C_2(T)D_{el}/d_{el}$. This result, combined with the functional box-counting technique, yields a direct method for estimating d_{el}, which we call "elliptical dimensional sampling" (Fig. 3). For each degree of stratification D_{el}, we measure $C_{D_{el}}(T_i)$ for all the thresholds T_i (the boxes here are of size L by L by L^{H_z}, with $D_{el} = 1 + 1 + H_z$). When we choose boxes with exactly the correct stratification (that is, $D_{el} = d_{el}$), then $C_{D_{el}}(T_i) = C_2(T_i)$ for all T_i. The method can be slightly improved statistically by determining the zero of the following function:

$$f(D_{el}) = \sum_{i=1}^{k} [C_{D_{el}}(T_i) - C_2(T_i)] \qquad (3)$$

where we have used the empirical $C_{D_{el}}$ and C_2 functions that were determined by functional box-counting. The sum is over the number of thresholds (nine in this case).

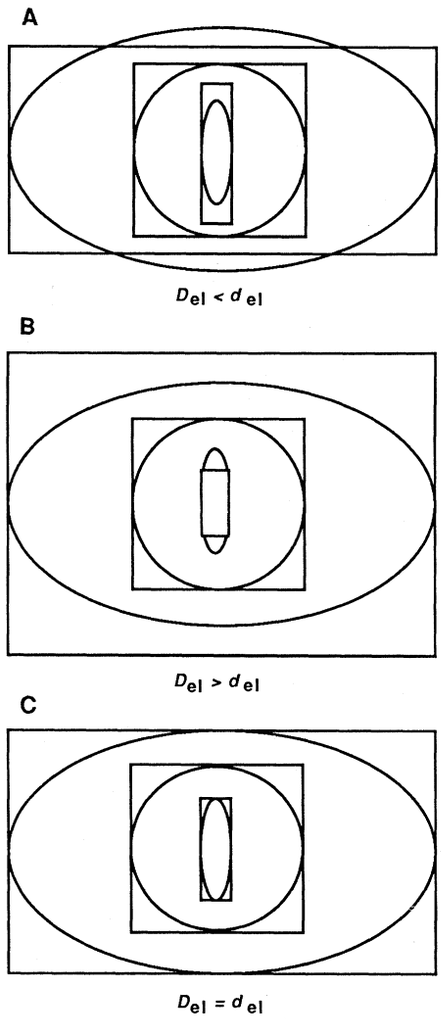

Fig. 3. Elliptical dimensional sampling. Average eddies at three different scales are represented by ellipses (dimension d_{el}); the boxes used to analyze the fields are shown as rectangles (dimension D_{el}). In (**A**) the boxes are too stratified. In (**B**) they are not stratified enough. In (**C**) they are correctly stratified ($D_{el} = d_{el}$).

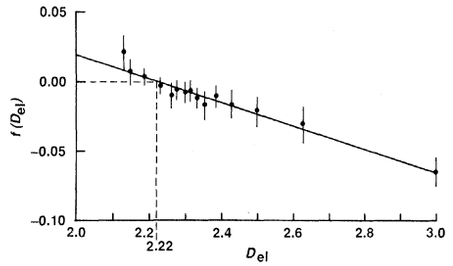

Fig. 4. The function $f(D_{el})$ as described in the text is the average of data taken from 20 scans, and is based on 15 different values of D_{el} and 9 reflectivity thresholds (for a total of $9 \times 15 \times 20 = 2700$ dimensions). Averages and standard deviations, indicated by the error bars, are plotted. The least-squares linear regression is shown and has a horizontal intercept ($D_{el} = d_{el}$) of 2.22.

Furthermore, the above formula for $C_{D_{el}}(T_i)$ shows that

$$f(D_{el}) = (D_{el}/d_{el} - 1)\sum_{i=1}^{k} C_2(T_i) \qquad (4)$$

Hence $f(D_{el})$ is linear.

Figure 4 shows the result as D_{el} is varied through 15 values between 3.0 and 2.13; the latter was the lowest value accessible with the data set [this corresponded to boxes of 1 by 1 by 1 pixel and boxes 190 by 190 by 2 pixels (twice the anisotropic scale), where $2.13 = 2 + \log 2/\log 190$]. The same nine thresholds were used as before. The function $f(D_{el})$ was determined separately on 20 radar rain fields; the linear regression shown yields $d_{el} = 2.22 \pm 0.07$. The error is the standard deviation of d_{el} estimated from each of the 20 scans separately. These scans were chosen at random from data from the Montreal region during summer of 1984, all on separate days. The individual slopes and axis intercepts varied by ±11 and ±9 percent, respectively, which indicated that any systematic variation is small.

An obvious application of this result is to quantitatively measure the stratification. For example, the rain field is considerably more stratified than the wind field, which has a value $d_{el} = 23/9 = 2.555\ldots$ that has been estimated from energy spectra and dimensional arguments (*6*). These elliptical dimensions are necessary in both additive (*8*) and multiplicative [cascade-type (*7, 9, 10, 22, 23*)] stochastic mesoscale modeling (*16*). In numerical weather prediction models, the calculated and empirical values of d_{el} can be compared to study the "stochastic coherence" (*24*) of the calculated values. When fields are stratified, efficient modeling and measurement procedures must involve choosing discrete vertical and horizontal scales that are "comparable"; the elliptical dimension gives us the required exponent. This poses interesting theoretical questions for dynamical models that involve interacting fields with different degrees of stratification.

REFERENCES AND NOTES

1. S. Lovejoy, *Science* **216,** 185 (1982).
2. D. Schertzer and S. Lovejoy, in *Proceedings of the Fourth Symposium on Turbulent Shear Flows* (University of Karlsruhe, West Germany, 1983), p. 11.18.
3. S. Lovejoy and D. Schertzer, in *Preprints, Sixth Symposium on Turbulence and Diffusion* (American Meteorological Society, Boston, 1983), p. 102; D. Schertzer and S. Lovejoy, in *Preprints, Fourth Conference on Atmospheric and Oceanic Waves and Stability* (American Meteorological Society, Boston, 1983), p. 58.
4. D. Schertzer and S. Lovejoy, in *Preprints, International Union of Theoretical and Applied Mechanics Symposium on Turbulence and Chaotic Phenomena in Fluids* (International Union of Theoretical and Applied Mechanics, Kyoto, Japan, 5 to 10 September 1983) p. 141.
5. ———, *Turbulence and Chaotic Phenomena in Fluids*, T. Tatsumi, Ed. (North-Holland, Amsterdam, 1984), p. 505.
6. ———, in *Turbulent Shear Flow*, L. J. Bradbury and F. Durst, Eds. (Springer, New York, 1985), vol. 4, pp. 7–33.
7. ———, *Phys. Chem. Hydrodyn.* **6,** 623 (1985).
8. S. Lovejoy and D. Schertzer, *Water Resour. Res.* **21,** 1233 (1985).
9. D. Schertzer and S. Lovejoy, *Fractals in Physics*, S. Pietronero and E. Tosatti, Eds. (North-Holland, Amsterdam, 1986), p. 457.
10. ———, *J. Geophys. Res.*, in press.
11. H. G. E. Hentschel and I. Proccacia, *Physica* **8D,** 435 (1983).
12. P. Grassberger, *Phys. Lett.* **97A,** 227 (1983).
13. U. Frisch and G. Parisi, in *Turbulence and Predictability in Geophysical Fluid Dynamics and Climate Dynamics*, M. Ghil, R. Benzi, G. Parisi, Eds. (North- Holland, Amsterdam, 1985), p. 84.
14. T. C. Halsey, M. H. Jensen, L. P. Kadanoff, I. Procaccia, B. I. Shraiman, *Phys. Rev. A* **33,** 1141 (1986).
15. S. Lovejoy and D. Schertzer, *Digital Image Processing in Remote Sensing*, J. P. Muller, Ed. (Francis and Taylor, London, in press), chap. 14.
16. ———, *Bull. Am. Meteorol. Soc.* **67,** 21 (1986).
17. ———, P. Ladoy, *Nature (London)* **319,** 43 (1986).
18. ———, *ibid.* **320,** 401 (1986).
19. P. Gabriel, S. Lovejoy, G. L. Austin, D. Schertzer, in *Preprints, Sixth Conference on Atmospheric Radiation* (American Meteorological Society, Boston, 1986), p. 230.
20. The standard error of the fits was computed. The maximum value for all the fits (the largest T was used) was ± 0.07.
21. B. Kerman, K. Szeto, S. Lovejoy, D. Schertzer, in *Preprints, Nonlinear Variability in Geophysics* (McGill University, Montreal, 1986), p. 34.
22. D. Schertzer and S. Lovejoy, *Ann. Math. Quebec* in press.
23. Multiplicative processes are required if we are to obtain the necessary hierarchy of fractal dimensions.
24. D. Schertzer *et al.*, in *Preprints, International Association of Meteorology and Atmospheric Physics and the World Meteorological Organization Symposium on the Maintenance of the Quasi-Stationary Components of the Flow in the Atmosphere and in Atmospheric Models*, (World Meteorological Organization, Geneva, 1983), p. 325.

25. We acknowledge discussions with G. L. Austin, P. Gabriel, V. K. Gupta, J. P. Kahane, P. Ladoy, D. Lavallée, E. Levitch, J. P. Muller, R. Peschanski, A. Saucier, T. Warn, E. Waymire, and J. Wilson. We thank the Aspen Center for Physics for their hospitality.

23 September 1986; accepted 6 January 1987

Foam Structures with a Negative Poisson's Ratio

RODERIC LAKES

A novel foam structure is presented, which exhibits a negative Poisson's ratio. Such a material expands laterally when stretched, in contrast to ordinary materials.

VIRTUALLY ALL COMMON MATERIals undergo a transverse contraction when stretched in one direction and a transverse expansion when compressed. The magnitude of this transverse deformation is governed by a material property known as Poisson's ratio. Poisson's ratio is defined as the negative transverse strain divided by the axial strain in the direction of stretching force. Since ordinary materials contract laterally when stretched and expand laterally when compressed, Poisson's ratio for such materials is positive. Poisson's ratios for various materials are approximately 0.5 for rubbers and soft biological tissues, 0.45 for lead, 0.33 for aluminum, 0.27 for common steels, 0.1 to 0.4 for typical polymer foams, and nearly zero for cork.

Negative Poisson's ratios are theoretically permissible but have not, with few exceptions, been observed in real materials. Specifically, in an isotropic material (a material that does not have a preferred orientation) the allowable range of Poisson's ratio is from −1.0 to +0.5, based on thermodynamic considerations of strain energy in the theory of elasticity (*1*). It is believed by many that materials with negative values of Poisson's ratio are unknown (*1*); however, Love (*2*) presented a single example of cubic "single crystal" pyrite with a Poisson's ratio of −0.14 and he suggested that the effect may result from a twinned crystal. Analysis of the tensorial elastic constants of anisotropic single crystal cadmium suggests that Poisson's ratio may attain negative values in some directions (*3*). Anisotropic, macroscopic two-dimensional flexible models of certain honeycomb structures (not materials) have exhibited negative Poisson's ratios in some directions (*4*). These known examples of negative Poisson's ratios all depend on the presence of a high degree of anisotropy; the effect only occurs in some directions and may be dominated by coupling between stretching force and shear deformation. The materials described in this report, by contrast, need not be anisotropic.

Foams with negative Poisson's ratios were

Department of Biomedical Engineering, University of Iowa, Iowa City, IA 52242.